

# An insight into the extraction of transition metal ions by picolinamides associated with intramolecular hydrogen bonding and rotational isomerization†

Cite this: *RSC Adv.*, 2014, 4, 29702

Yan Li,<sup>a</sup> Yiming Jia,<sup>a</sup> Zhenwen Wang,<sup>a</sup> Xianghui Li,<sup>a</sup> Wen Feng,<sup>a</sup> Pengchi Deng<sup>\*b</sup> and Lihua Yuan<sup>\*a</sup>

The clear connection between molecular structures of *N*-substituted picolinamides and extraction behaviour has been rationalized by highlighting the relationship between intramolecular hydrogen bonding and rotational isomerism. To this aim aromatic pyridine-2,6-dicarboxamides **1a–1c** with *N*-substitution and their analogues **3a** and **3b** containing intramolecular hydrogen bonds were designed and synthesized. The results from the liquid–liquid extraction towards some representative transition metal picrates including Ag<sup>+</sup>, Hg<sup>2+</sup>, Pb<sup>2+</sup>, Cd<sup>2+</sup>, Zn<sup>2+</sup>, Cu<sup>2+</sup>, Co<sup>2+</sup> and Ni<sup>2+</sup> salts demonstrated that the higher selectivity and efficiency towards Hg<sup>2+</sup> (88.6–95.4%) over other metal cations stem mainly from *N*-substitution *via* disruption of intramolecular H-bonding. X-ray structural analysis, and ordinary and variable-temperature proton and carbon NMR experiments provided supporting information for expounding the difference in extraction ability among these ligands, particularly the importance of *N*-substitution that leads to the formation of rotamers affecting the extraction process.

Received 8th March 2014  
Accepted 19th June 2014

DOI: 10.1039/c4ra02030h

www.rsc.org/advances

## Introduction

Amide-based compounds and their corresponding metal complexes have been widely investigated due to the easy synthesis of ligands, high resistance to hydrolysis, and potential coordination ability of amide hydrogen and/or oxygens.<sup>1</sup> These features render them find applications as extractants in separation technology,<sup>2</sup> sensors in detecting metal ions,<sup>3</sup> and building blocks for constructing architectures in catalysis.<sup>4</sup> Diglycolamides,<sup>5</sup> pyridine-modified calixarenes,<sup>6</sup> CMPO-tripodands,<sup>7</sup> and pyridine dicarboxamides<sup>8</sup> are examples of extraction systems that have demonstrated higher separation efficiency in discriminating lanthanides/actinides (Ln/Act) elements. Among them, pyridine-based carboxyamides or dicarboxyamides and their analogues represent a class of ligands that have attracted attention in forming metal complexes<sup>9</sup> and in use for metal separation.<sup>8,10</sup> The amide linkages, as part of the molecular constituents of these ligands

or complexes, were found to involve in interacting or coordinating with metal ions in synergy with the nitrogen of pyridine moiety.<sup>9,11</sup> It has been noted that substitution on nitrogen of amide bonds of synthetic ligands led to improved performance in two-phase extraction of lanthanides/actinides elements.<sup>12</sup> In fact, the effect of *N*-substituted ligands upon the extraction and separation efficiency had been observed in diamide systems *ca.* two decades before.<sup>13</sup> However, the reason behind it is still not clearly clarified. For 2,6-dicarboxypyridine diamides, the explanation was limited to the electronic and steric effects that may dominate the atoms coordinating to the metal center in.<sup>14</sup>

It was known that hydrogen bonding formation involving amide groups contribute a great deal to the construction of complex natural and artificial supramolecular assemblies.<sup>15</sup> Incorporation of hydrogen bond (H-bond) groups into ligands was able to orient incoming groups or stabilize metal–ligand adducts.<sup>16</sup> Besides the importance of metal complexing sites associated with amide linkage for effecting the separation process, intra- or intermolecular hydrogen bonding contained in the molecular structure of a ligand may also play a role in governing the extraction efficiency and selectivity. However, this aspect has scarcely been explored to date. We recently employed hydrogen bonded aromatic oligoamides with backbones pre-organized by aid of intramolecular three-center hydrogen bonds for solvent extraction separation of transition metal ions.<sup>17</sup> The importance of intramolecular hydrogen bonding present in these compounds was also demonstrated by the formation of

<sup>a</sup>College of Chemistry, Key Laboratory for Radiation Physics and Technology of Ministry of Education, Institute of Nuclear Science and Technology, Sichuan University, Chengdu 610064, China. E-mail: lhyuan@scu.edu.cn; Fax: +86-28-85418755; Tel: +86-28-85416996

<sup>b</sup>Analytical & Testing Center, Sichuan University, Chengdu 610064, China. E-mail: pcdeng@yahoo.com

† Electronic supplementary information (ESI) available: Characterization details, extraction data. CCDC 990530 and 990531. For ESI and crystallographic data in CIF or other electronic format see DOI: 10.1039/c4ra02030h

their corresponding cyclo[6]aramides<sup>18</sup> and efficiency in extraction towards Ln/An elements.<sup>19</sup> Based on similar pre-organization-induced folding mechanism, their higher aromatic amide polymers also exhibited selective extraction of thorium(IV) and rare earth elements.<sup>20</sup> Very recently, we revealed that the subtle change of the coordination environment made by local intramolecular H-bonding of CMPO-modified calixarenes led to selective separation of light/heavy lanthanides and group separation between lanthanides and thorium/uranium.<sup>21</sup> Despite much progress made in using 2,6-pyridine dicarboxyamides as solvent extractants<sup>22</sup> and the well-known fact for the formation of amide rotamers,<sup>23</sup> surprisingly, the correlation between the presence of intramolecular hydrogen bonding associated with amide NH in effecting liquid–liquid extraction behaviour and rotational isomerization is still unexplored.

With our continued interest in amide-based compounds and macrocyclic compounds for metal ion separation,<sup>24</sup> we report herein on the exploration of intramolecular hydrogen bonding in regulating extraction process pertinent to rotational isomerism by *N*-substitution using a series of synthesized picolinamides. Transition metal ions including Ag<sup>+</sup>, Hg<sup>2+</sup>, Pb<sup>2+</sup>, Cd<sup>2+</sup>, Zn<sup>2+</sup>, Cu<sup>2+</sup>, Co<sup>2+</sup>, Ni<sup>2+</sup> were selected to assess the outcome due to structural alternation of ligands used in the liquid–liquid extraction experiments.

## Results and discussion

### Initial consideration and molecular design

Picolinamides **1**–**3** were used in the present study (Scheme 1). Initially compound **1a** bearing alkoxy substituents was designed as a control for ligand **2** in comparing extraction of transition metal ions. Compound **2** was reported to be potential extractant for minor actinides<sup>25</sup> and palladium separation.<sup>26</sup> Interestingly, examination of <sup>1</sup>H NMR spectrum of **1a** showed a complicated pattern comprising several sets of signals that cannot be designated as a pure component. However, a base peak at *m/z* 490.2701 corresponding to the most abundant species [M + H]<sup>+</sup> in HRMS spectrum and a single peak from HPLC experiments excluded the possibility of the presence of any other impurities

(see ESI†). Thus, the most likely possibility is the presence of rotational isomers for **1a** since rotation around the amide bonds are considerably hindered upon introducing an ethyl group onto the amidic nitrogen. In other words, it is the coexistence of several conformational isomers that caused the complexity of its NMR spectrum. This led to the design of compound **3a** without substitution on nitrogen atoms. At the same time, propoxy groups in **3a** are placed at *ortho*-position adjacent to the amide bond to allow formation of intramolecular hydrogen bonds, thus partially rigidifying the backbone of the molecule (*vide post*). Free rotation around nitrogen of the amide NH and carbon of the phenyl ring is expected to be impossible. Compound **3b**, which bears the same backbone with *ortho*-substituted methyl group, is designed to see if partial hydrogen bonding is still strong enough to maintain the molecular conformation as **3a**. Positional isomers **1b** and **1c** are also designed for comparison. Given the importance of coordination directionality in forming extractive species, it can be envisioned that if the orientation of carbonyl oxygen atoms is manipulated by the presence of hydrogen bonding to restrict the amide rotations, different extraction behaviour should result.

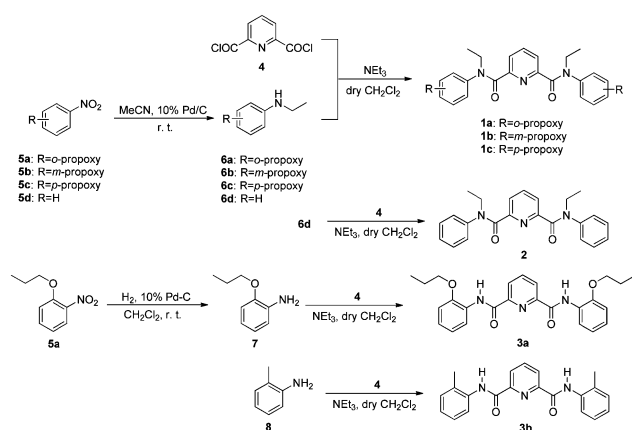
### Synthesis and solid state structures

Typically all 2,6-pyridine dicarboxyamides **1a**–**1c**, **2**, **3a** and **3b** were synthesized based on the coupling reactions of acyl chlorides and corresponding anilines according to Scheme 1. All of these compounds were characterized by <sup>1</sup>H NMR, <sup>13</sup>C NMR and HRMS. Compound **2** was prepared according to the reported procedure.<sup>25a</sup>

The key precursors **5a**–**5c** were obtained by reaction of commercially available hydroxyl group-substituted nitrobenzene and propyl bromide in the presence of K<sub>2</sub>CO<sub>3</sub>. The syntheses of **6a**–**6c** were carried out employing MeCN as ethylation agent.<sup>27</sup> Treating the *N*-alkylated aniline derivatives **6a**–**6c** with **4** resulted in **1a**, **1b**, and **1c** in overall isolated yields of 82%, 92% and 88%, respectively. Compound **3a** was readily prepared in 81% yield *via* two steps from hydrogenation of **5a** with Pd/C as catalyst to afford **7**, followed by coupling of 2,6-pyridinedicarbonyl dichloride **4**.

Single crystals of ligands **1a** and **3a** were obtained by slow evaporation of a solution of CH<sub>2</sub>Cl<sub>2</sub>/*n*-hexane and ethyl acetate/*n*-hexane at room temperature, respectively. Selected bond lengths and angles for the two ligands from X-ray diffraction experiment are given in Table 1.

Fig. 1a shows a view of the molecular structure of **1a**. The molecule of **1a** has a C<sub>2</sub> symmetry, and the C<sub>2</sub> axis passes through atoms C1 and N1 of the pyridine ring. The atoms of the amide groups and those connected to amide carbon and nitrogen (O1, C3, C4, N2, C5 and C7) are almost in a plane. The mean deviation from plane is 0.0401 Å. In addition, the bond angles across the amide nitrogen, C4–N2–C5, C4–N2–C7 and C5–N2–C7 are all approximately 120°. These data suggest the sp<sup>2</sup> hybridization of the amide nitrogens N2, and the considerable double bond character for the OC–N amide bonds.<sup>11a,28</sup> So far as the arrangement of amide nitrogen relative to pyridine



Scheme 1 Synthesis of 2,6-pyridine dicarboxyamides **1a**–**1c**, **2**,<sup>25a</sup> **3a** and **3b**.

Table 1 Selected bond lengths (Å) and angles (°) for **1a** and **3a**

	Bond lengths (Å)		Bond angles (°)	
<b>1a</b>	C3–C4	1.510(5)	C3–C4–O1	119.82(5)
	O1–C4	1.222(7)	C3–C4–N2	117.63(2)
	N2–C4	1.349(0)	O1–C4–N2	122.53(2)
	N2–C5	1.474(5)	C4–N2–C5	119.12(8)
	N2–C7	1.431(5)	C4–N2–C7	122.92(6)
<b>3a</b>	C10–C11	1.507(8)	C11–C10–O2	121.75(7)
	C10–O2	1.218(6)	C11–C10–N1	113.35(3)
	C10–N1	1.347(6)	O2–C10–N1	124.89(0)
	N1–H1	0.859(7)	C10–N1–H1	116.28(5)
	N1–C9	1.408(2)	C10–N1–C9	127.52(0)
	C16–C15	1.499(8)	H1–N1–C9	116.19(5)
	C16–O3	1.211(2)	C15–C16–O3	122.05(9)
	C16–N3	1.351(2)	C15–C16–N3	113.68(6)
	N3–H3	0.859(8)	O3–C16–N3	124.25(2)
	N3–C17	1.404(5)	C16–N3–H3	115.96(5)
			C16–N3–C17	128.08(5)
			H3–N3–C17	115.95(0)

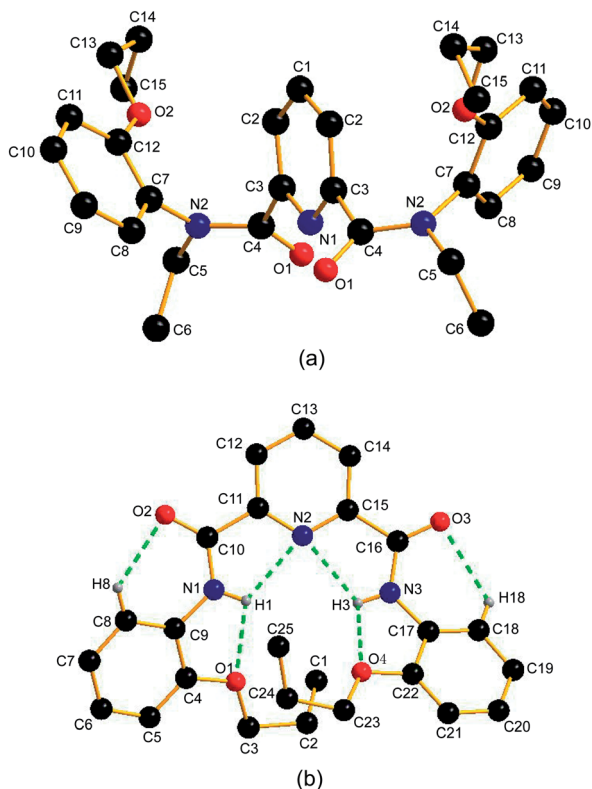


Fig. 1 The crystal structures of (a) **1a** and (b) **3a**. Hydrogen atoms are omitted for the sake of clarity except for those forming hydrogen bonds.

nitrogen is concerned, the crystal structure of **1a** reveals the *anti-anti* conformation: both of the amide nitrogens placed in *trans* position with respect to pyridine nitrogen. The dihedral angle between the pyridine ring and each of the amide planes is 64.99(5)°. To avoid n–n repulsion between the lone pairs of carbonyl oxygens, the two amide planes are staggered away

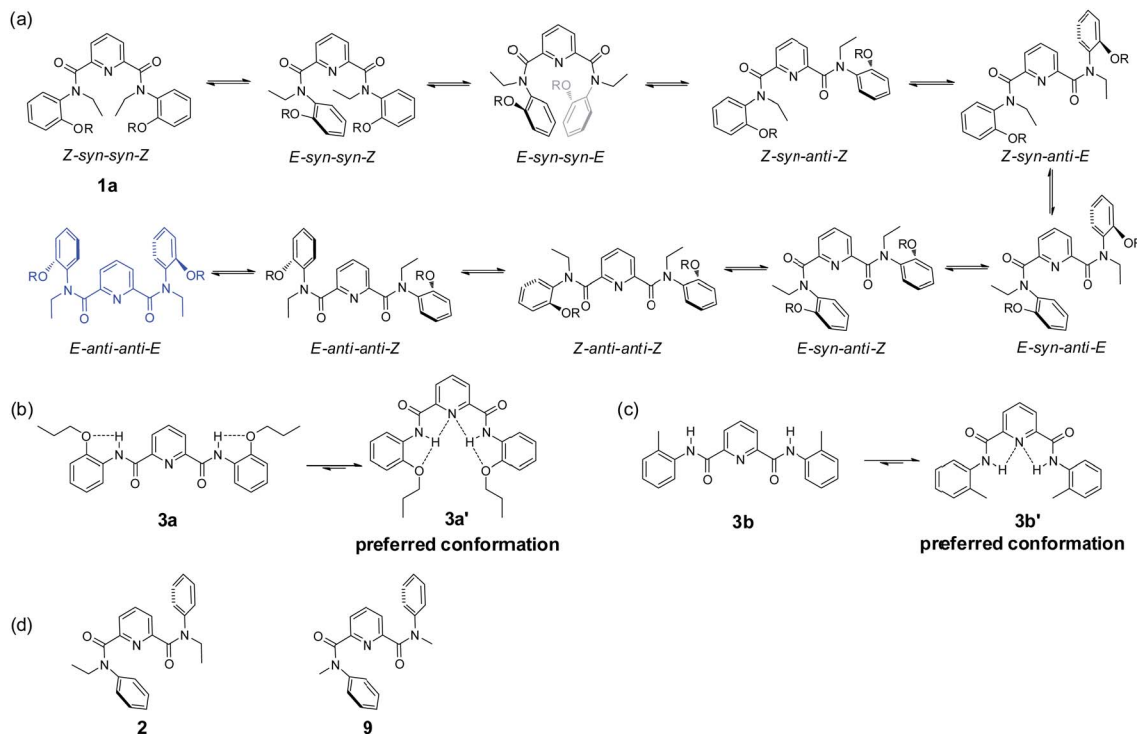
from each other with a dihedral angle of 75.65(4)°. The orientation of the phenyl group is designated as *E (trans)* relative to the carbonyl oxygens when the OC–N amide bond is considered as a double bond. Consequently, **1a** adopts *E-anti-anti-E* conformation (also see Scheme 2a, blue). The dihedral angle between the pyridine ring and each of the two phenyl groups (C7–C8–C9–C10–C11–C12) is 65.04(7)°.

For **3a**, the solid state structure clearly indicates the presence of two intramolecular three-center hydrogen bonds, N2⋯H1⋯O1 and N2⋯H3⋯O4, each comprising two five-membered rings to fix the molecule in a crescent fashion as shown in Fig. 1b. The parameters of H-bonds involving in **3a** are shown in Table 2. The H-bond lengths of N2⋯H1, O1⋯H1, N2⋯H3 and O4⋯H3 are 2.219(7) Å, 2.277(6) Å, 2.223(5) Å and 2.254(9) Å, respectively, suggesting the formation of strong H-bonds. Two additional weak hydrogen bonds O2⋯H8 and O3⋯H18 are also observed,<sup>29</sup> the lengths of which are 2.464(5) Å and 2.424(0) Å, respectively. The dihedral angles between the pyridine ring and phenyl groups C4–C5–C6–C7–C8–C9 (phenyl 1) and C17–C18–C19–C20–C21–C22 (phenyl 2) are 32.43(4)° and 25.46(4)°, respectively. It is worth noting that the two intramolecular three-center H-bonds are twisted and not in the same plane due to the steric crowding between the two adjacent propoxy groups. As in **1a**, the two amide nitrogens in **3a** are also sp<sup>2</sup> hybridized for the bond angles across each of the two amide nitrogens N1 and N3 are *ca.* 120° and the mean deviations of the two amide group C9–N1–H1–C10–O2–C11 (plane 1) and C15–C16–O3–N3–H3–C17 (plane 2) are 0.0341 and 0.0417, respectively. The dihedral angles between the pyridine ring and the amide groups plane 1 and plane 2 are 5.39(1)° and 2.46(3)°, respectively.

A similar compound with methoxy groups, *N,N'*-bis-(2-methoxyphenyl)pyridine-2,6-dicarboxamide, gave a crystal structure analogous to **3a** where two three-center H-bonds were also observed.<sup>29a</sup>

### Intramolecular hydrogen bonds (H-bonds) in solution

Infrared spectrum could only provide evidence of hydrogen bond of **3** in CHCl<sub>3</sub> (see ESI, Fig. S24 and S26†), but it is impossible to distinguish intramolecular from intermolecular hydrogen bonding interactions. The bands due to hydrogen bonded NH stretching of **3a** and **3b** were found to shift towards lower wavenumber of respective 3372 and 3397 cm<sup>-1</sup> compared to higher wavenumber of more than 3400 cm<sup>-1</sup> of common free amide NH.<sup>30a</sup> Thus, to verify the presence of intramolecular H-bonds in picolinamides **3** without *N*-substitution, the temperature coefficients  $d\delta_{\text{H}}/dT$  of N–H were determined in the temperature range between 298 K to 333 K (in steps of 5 K) in CDCl<sub>3</sub> or DMSO-*d*<sub>6</sub>/CDCl<sub>3</sub> (2/8, v/v) by variable-temperature <sup>1</sup>H NMR experiments (Fig. 2). It is generally accepted that in nonpolar solvents when the coefficient is less negative than –3 ppb K<sup>-1</sup>, the hydrogen bonding interaction is considered as intramolecular; when it is more negative than –5 ppb K<sup>-1</sup>, it is taken as intermolecular hydrogen bond.<sup>30</sup> The  $d\delta_{\text{H}}/dT$  of N–H in **3a** was measured to be –1.58 ppb K<sup>-1</sup> in DMSO-*d*<sub>6</sub>/CDCl<sub>3</sub> (2/8, v/v), which shows a small variation with temperature. This suggests the high possibility of the presence of intramolecular



Scheme 2 Conformational conversion of isomers (a)–(c): (a) rotamer interconversion from **1a**; (b) conformer formation of **3a** via intramolecular H-bonding; (c) conformer formation of **3b** via intramolecular H-bonding. (d) Conformation of compounds **2** (ref. 11a) and **9** (ref. 35) in solid state.

Table 2 The parameters of H-bonds involving in **3a**

D	H	A	$d(\text{H}\cdots\text{A})/\text{\AA}$	$\angle \text{D-H}\cdots\text{A}/^\circ$
N1	H1	N2	2.219(7)	111.59(1)
N1	H1	O1	2.277(6)	101.14(1)
N3	H3	N2	2.223(5)	111.30(9)
N3	H3	O4	2.254(9)	103.11(2)
C8	H8	O2	2.464(5)	112.99(0)
C18	H18	O3	2.424(0)	114.78(2)

H-bonds even in a polar solvent.<sup>31</sup> Therefore, these results are in accord with the observation of presence of intramolecular H-bonds in the crystal structure of **3a**. For **3b**, the  $d\delta_{\text{H}}/dT$  of N-H was measured to be  $-1.62$  ppb  $\text{K}^{-1}$  in nonpolar  $\text{CDCl}_3$  and  $-5.71$  ppb  $\text{K}^{-1}$  in polar solvent  $\text{DMSO-}d_6/\text{CDCl}_3$  (2/8, v/v). The small variation of  $d\delta_{\text{H}}/dT$  in nonpolar solvent also discloses the presence of intramolecular H-bonds in **3b**. Both of the infrared spectra and temperature coefficients data indicate that the two-center hydrogen bonds in **3b** are less stable than the three-center hydrogen bonds in **3a**.

### Rotational isomerization

Comparison of the  $^1\text{H}$  NMR spectra of compounds **1a–1c** and **3a** or **3b** disclosed a significant difference in complicity of signal patterns and chemical shifts of protons b and a on the pyridine moiety (Fig. 3).

Among the three positional isomers **1a–1c**, **1a** exhibits the most poorly-resolved signals over the full spectrum (Fig. 3a). We exclude the possibility of contamination of impurities by HPLC and MS detection (see ESI<sup>†</sup>). Compound **2**, a well-known extractant<sup>25,26</sup> with *N*-ethylated substituent, but free of any replacement on benzene ring, showed similar indistinguishable signals (see ESI<sup>†</sup>). In stark contrast, **1c**, which bears a propoxy group at *para*-position, provided a much “clean” spectrum with distinguishable signals for almost all aromatic and aliphatic protons a  $\sim$  i (Fig. 3c). Apart from the major clear signals, there are some signals of very low intensity, suggestive of the presence of other rotational isomers. For **1b**, the situation sits in between **1a** and **1c** (Fig. 3b). Signals of each proton from various

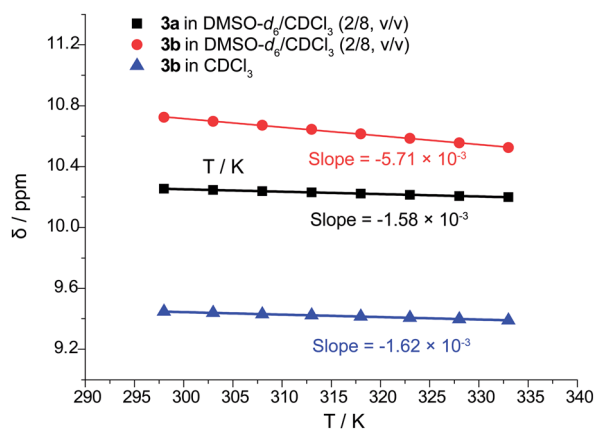


Fig. 2 Chemical shifts of NH in **3a/3b** versus temperature in  $\text{DMSO-}d_6/\text{CDCl}_3$  (2/8, v/v) or  $\text{CDCl}_3$  (600 MHz, 298 K to 333 K).

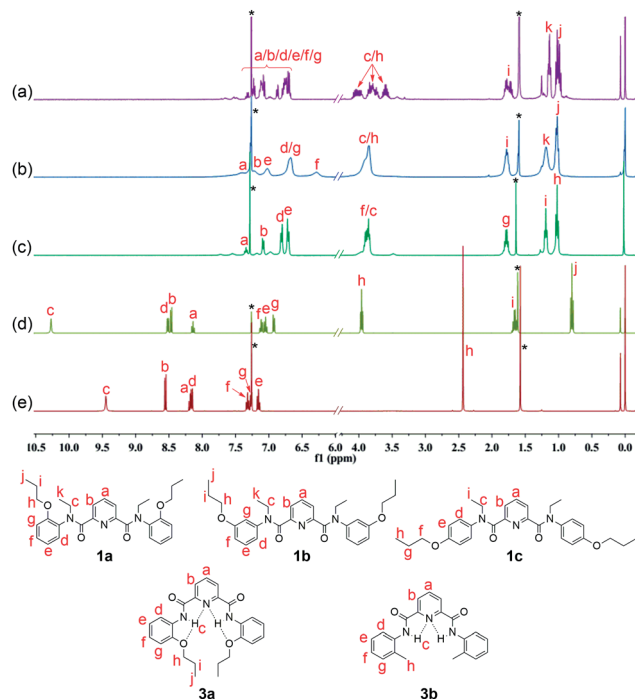


Fig. 3  $^1\text{H}$  NMR spectra of compounds (a) **1a**, (b) **1b**, (c) **1c**, (d) **3a** and (e) **3b** in  $\text{CDCl}_3$  (400 MHz, 298 K). Sign "\*" represents signals of solvents.

rotamers of **1b** show a tendency to coalesce together but are broad. If compared to the clear, well-resolved signals for **3a** (Fig. 3d), these observations strongly suggest that the spectral complexity of **1a** is more likely to arise from the concurrent rotamers, rotational isomers that result from the hindered rotations about OC–N bonds and N (amide)–C (Ph).<sup>23b,32</sup> It should be noted that the molecular skeleton of **3a** is preorganized by aid of intramolecular three-center hydrogen bonds to take a crescent conformation. The two localized intramolecular hydrogen bonds each consist of two S(5)-type rings that involve the backbone amide hydrogen. It has been well established that this three-center hydrogen bond is highly stable, the presence of which hinders the rotational freedom of the aromatic amide-based backbones.<sup>33</sup> Therefore, the shape-persistency endows the molecule of **3a** with drastically-reduced rotation with respect to **1a–1c** in solution, leading to an indication of presence of only one species in solution in  $^1\text{H}$  NMR spectrum. Furthermore, the rigid backbone also renders the preorganized carbonyl oxygen atoms of the molecule point outwards in **3a**. Similarly, the presence of two intramolecular hydrogen bonds in **3b** also enforces globally curved conformation of the molecular backbone,<sup>23b,34</sup> thus hindering the rotation about OC–N amide bond as manifested in its clear proton signals (Fig. 3e).

The difference of  $^{13}\text{C}$  NMR spectra (Fig. 4) among **1a–1c**, **3a** and **3b** was also observed. If there is no presence of rotational isomers in **1a–1c**, with the molecular formula  $\text{C}_{29}\text{H}_{35}\text{N}_3\text{O}_4$ , the number of signals should be equal to or less than 15 due to their structural symmetry. In fact, there are totally 29 strong signals in  $^{13}\text{C}$  NMR spectrum of **1a** along with some very weak signals

across the full spectrum that could be detected (Fig. 4a), suggesting the presence of a mixture of several major and minor rotamers in solution. This is consistent with the observation of several sets of indistinct  $^1\text{H}$  NMR signals (Fig. 3a). With **1b**, a structural isomer of **1a** with propoxy groups at *meta*-position of the benzene ring, the number of signals in  $^{13}\text{C}$  NMR spectrum is drastically decreased to only 15, but some of the signals are broad (Fig. 4b). Compound **1c**, which bears a *para*-substituent, gives a spectrum containing only 13 signals along with another set of very weak signals (Fig. 4c). The decreased number of signals from  $^{13}\text{C}$  NMR data suggests that the rotational barrier decreases with change of substituents from *ortho* to *meta* to *para* position. This is different from the result from **3a** and **3b** where only well-resolved 13 and 11 signals were observed (Fig. 4d and e), respectively, corresponding exactly to respective 25 and 23 carbons in the molecules due to their shape-persistency of molecular backbone rigidified by intramolecular hydrogen bonds. These results agree well with those from  $^1\text{H}$  NMR spectra. Given the fact that the formation of rotamers is caused by the limitation of CO–N bond rotation, reduction of steric hindrance *via* alternation of substitution position would lead to decreased rotational barrier and thus simple NMR patterns. Indeed, as the steric hindrance between alkoxyphenyl group and N–Et group increases with the substitution position in order of *ortho* > *meta* > *para*, the signals in both  $^{13}\text{C}$  and  $^1\text{H}$  NMR change from complex to simple and well-resolved.

To further probe rotational isomerization, variable-temperature NMR spectra were recorded using  $\text{DMSO}-d_6$  solutions of **1a** as a typical example in the temperature range from 298 K to 428 K (in steps of 10 K) for  $^1\text{H}$  NMR and 298 K to 418 K (in steps of 20 K) for  $^{13}\text{C}$  NMR. In  $^1\text{H}$  NMR spectra (Fig. 5), each proton of **1a** presents complicated multiple sets of signals resulting from various rotamers in solution at 298 K. Owing to the overlapping of signals, it is difficult to identify the species and calculate equilibrium ratio for the rotamer mixture. With the increase of temperature, all the signals in **1a** coalesce from complex to broad into a set of distinguishable signals at approximate 408 K. In  $^{13}\text{C}$  NMR spectra (Fig. 6), the number of the signals of **1a** decreased from 29 at 298 K to 15 at about 398 K due to coalescence effect. Based on the overall change from both  $^1\text{H}$  NMR and  $^{13}\text{C}$  NMR, the coalescence temperature for **1a** is reasonably set at approximately 408 K. It is not possible to calculate the temperature coefficients and the free energy, enthalpy and entropy of activation for the interconversion between each rotamers by Eyring analysis because of the complexity of  $^1\text{H}$  NMR in **1a**.

To clearly describe rotational isomerization, conformation designation is denoted by *Z*, *E*, *syn* and *anti*, respectively (*vide supra*). For **1a**, there should exist about ten typical rotational isomers theoretically due to the blocked rotations about the OC–N amide bonds and OC–C (pyridine) bonds (Scheme 2a), which explains undistinguished signals on the NMR timescale. The molecular structure of **1a** in the solid state confirms the exclusive formation of the *E-anti-anti-E* isomer. The two amide nitrogens are in *anti* conformation with respect to pyridine nitrogen. This is quite different from the solid state structure of the previously reported analogue **2** (ref. 11a) or **9** (ref. 35)

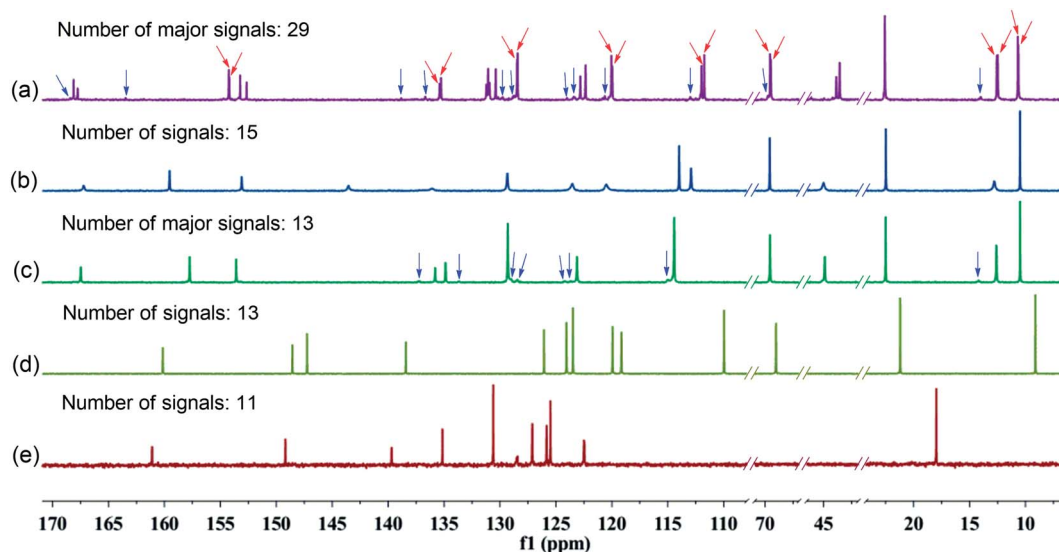


Fig. 4  $^{13}\text{C}$  NMR spectra of compounds (a) **1a**, (b) **1b**, (c) **1c**, (d) **3a** and (e) **3b** in  $\text{CDCl}_3$  (100 MHz, 298 K). Red and blue arrows represent some of the major and minor rotational isomers, respectively.

bearing no substituents where the *E-anti-syn-E* conformation was observed (Scheme 2d). In both cases of **1a** and **2** (or **9**), the *E* conformation as designated around amide bond is mainly attributed to the outcome of  $n-\pi$  repulsion, *i.e.*, electronic repulsion between the electron-dense center of the amide oxygen and the phenyl ring.<sup>28c,36</sup> Computer modeling<sup>37</sup> disclosed the higher energy for *anti-Z* conformation among four possible

combinations: *anti-Z*, *anti-E*, *syn-Z*, and *syn-E*, from which only six reasonable conformations *E-syn-syn-E*, *E-anti-syn-E*, *E-anti-anti-E*, *E-anti-syn-Z*, *E-syn-syn-Z*, *Z-syn-syn-Z* were obtained (Fig. 7). In the *anti-Z* conformation, carbonyl oxygen atoms experience both  $n-n$  repulsion with the pyridine nitrogen and  $n-\pi$  repulsion with the phenyl ring, leading to much lower stability of the conformation. Thus, the observed *E-anti-anti-E*

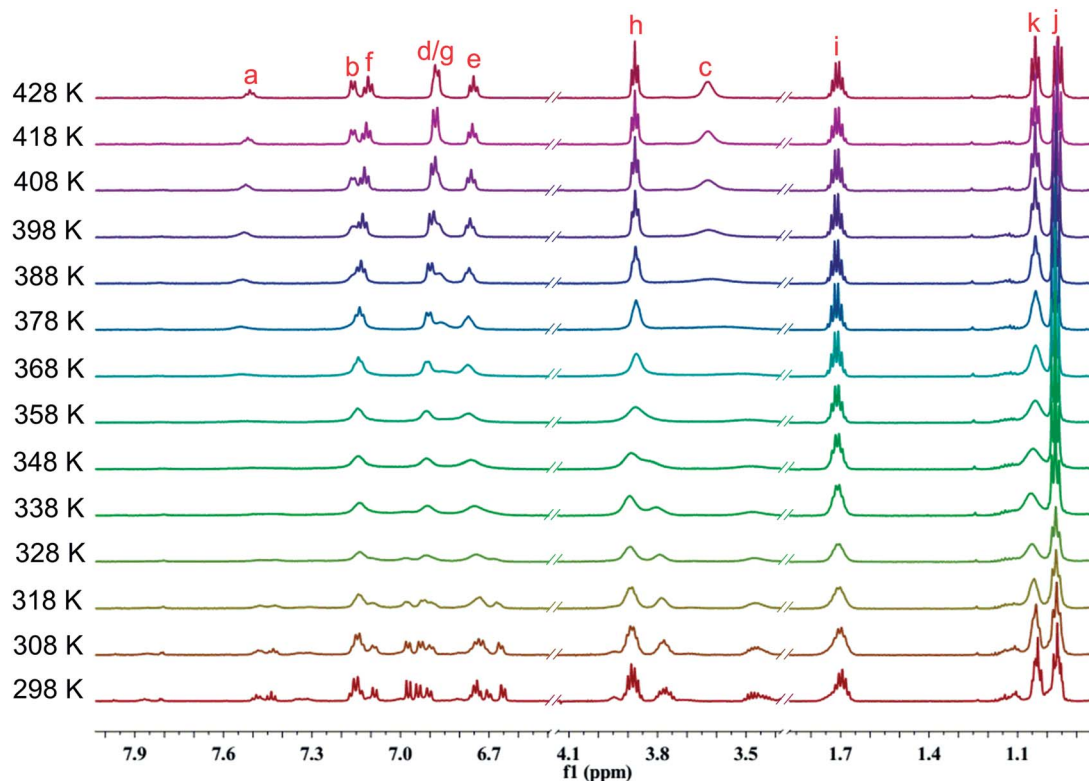


Fig. 5 Temperature dependent  $^1\text{H}$  NMR spectra of **1a** in  $\text{DMSO}-d_6$  in the range from 298 K to 428 K (600 MHz).

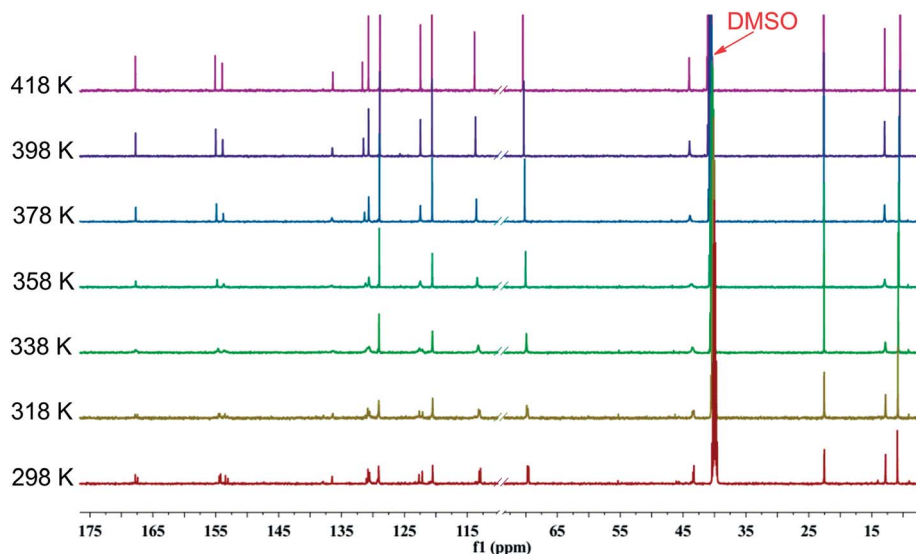


Fig. 6 Temperature dependent  $^{13}\text{C}$  NMR spectra of **1a** in  $\text{DMSO}-d_6$  in the range from 298 K to 418 K (150 MHz).

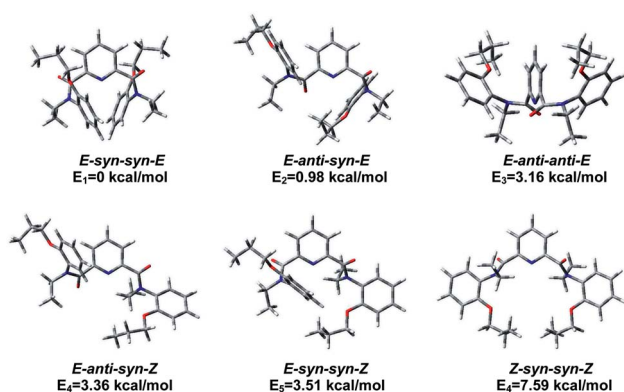


Fig. 7 Optimized rotational structures of compound **1a** obtained by DFT calculation at the B3LYP/6-31G(d) level.

conformation (**1a**) in the solid state is consistent to one of the calculated results.

### Liquid-liquid extraction

The structural difference between **1a** and **3a** is indeed manifested in the following extractive results.

Eight transition metal picrates were employed in liquid-liquid extraction experiments including picrate salts of  $\text{Ag}^+$ ,  $\text{Hg}^{2+}$ ,  $\text{Pb}^{2+}$ ,  $\text{Cd}^{2+}$ ,  $\text{Zn}^{2+}$ ,  $\text{Cu}^{2+}$ ,  $\text{Co}^{2+}$  and  $\text{Ni}^{2+}$ . The extraction abilities of picolinamides **1a-1c**, **2**, **3a** and **3b** towards these metal ions were examined by the standard picrate extraction method.<sup>38</sup> Compound **2** bearing no substituent on benzene rings was employed as a control for **1a-1c**.

Results from extraction of the above transition metal ions from water into dichloromethane are shown in Table 3 and Fig. 8. All ligands exhibited good to excellent extraction ability for  $\text{Hg}^{2+}$ . Almost no extraction or small extraction (<9%) was detected for  $\text{Pb}^{2+}$ ,  $\text{Cd}^{2+}$ ,  $\text{Zn}^{2+}$ ,  $\text{Co}^{2+}$  and  $\text{Ni}^{2+}$  except for **1a** for

$\text{Cu}^{2+}$ . Ligand **1a** extracted almost exclusively  $\text{Hg}^{2+}$  compared to other ions. Particularly noteworthy is the remarkable difference in extraction of  $\text{Hg}^{2+}$  with ligand **3a** containing intramolecular H-bonds and its *N*-substituted analogues **1a-1c**. For example, ligand **1a** showed extractability of 95.4% for  $\text{Hg}^{2+}$ , while **3a** gave a lower value of 38.4%. The large difference (57.0%) for **1a** as compared to **3a** is also revealed in **1b** and **1c**, which enhanced the extraction by 50.2% and 54.6%, respectively. Compound **2**, also ethylated on amide nitrogens, behaved in a similar fashion and showed a relatively large difference of 38.6% in extracting  $\text{Hg}^{2+}$  compared to **3a**. In principle, effective coordination of the ligand with metal ions requires the orientation of two carbonyl oxygen atoms and nitrogen of the pyridine moiety to be arrayed on the same side.<sup>9d,39</sup> For **3a**, orientation of carbonyl oxygens inwards in line with the pyridine nitrogen is impossible due to rigidified backbone by intramolecular hydrogen bonds. However, driven by the presence of metal ions transferred from the aqueous phase in the course of extraction, rotation of carbonyl oxygens to direct right coordination is more likely to occur for **1a-1c** even for rotamers of high energy (e.g., *E-syn-syn-Z*, *Z-syn-syn-Z*) since the intramolecular H-bonding was disrupted in **1a-1c** after ethylation of amide nitrogen. This explains the higher extractability of  $\text{Hg}^{2+}$  for these compounds (88.6–95.4%) compared to **3a** (38.4%). In fact, use of another compound **3b** containing two intramolecular hydrogen bonds afforded an extractability of 40.6% for  $\text{Hg}^{2+}$ , which is very close to that with **3a** as extractant. This indicates that intramolecularly hydrogen-bonded extractants (**3a** and **3b**) are inferior to those containing no hydrogen bonds, underscoring the importance of released constraint of rotational restriction for chelating metal ions upon extraction.

On the other hand, *N*-substituted groups can increase the basicity, nucleophilicity and softness of the coordinating amide groups and the lipophilicity of the extracted complex compared to *N*-H groups, which would also be one of reasons to enhance the extractability of **1a-1c** and **2**.<sup>40</sup> As shown in Table 3, the

Table 3 The extractability of aqueous metal picrates for compounds **1a–1c**, **2**, **3a** and **3b** into dichloromethane<sup>a</sup>

Metal ion	Hydration energy <sup>41</sup> $\Delta G_{\text{hyd}}$ (kJ mol <sup>-1</sup> )	Extraction <sup>b</sup> (%)					
		<b>1a</b>	<b>1b</b>	<b>1c</b>	<b>2</b>	<b>3a</b>	<b>3b</b>
Hg <sup>2+</sup>	-1760	95.4 ± 0.4	88.6 ± 1.0	93.0 ± 0.4	77.0 ± 0.5	38.4 ± 0.4	40.6 ± 0.2
Ag <sup>+</sup>	-430	58.7 ± 0.6	38.5 ± 0	42.1 ± 0.2	27.4 ± 0.4	2.9 ± 0.2	3.2 ± 0.2
Cu <sup>2+</sup>	-2010	31.5 ± 0.4	1.9 ± 0.2	2.1 ± 0.4	3.3 ± 0.7	1.5 ± 0.2	3.0 ± 0.7
Ni <sup>2+</sup>	-1980	8.2 ± 0.2	1.5 ± 0.2	0.5 ± 0.5	2.6 ± 0.5	0.9 ± 0.2	2.5 ± 0.2
Cd <sup>2+</sup>	-1755	3.0 ± 0.5	0.8 ± 0.9	0.6 ± 0.5	3.1 ± 0.3	0.7 ± 0	1.2 ± 0.2
Co <sup>2+</sup>	-1915	4.9 ± 0	0.8 ± 0.9	0.9 ± 0.2	0.2 ± 0.4	1.2 ± 0.2	3.3 ± 0.7
Zn <sup>2+</sup>	-1955	7.2 ± 0.5	0.3 ± 0.5	0.6 ± 0.2	1.9 ± 0.7	2.2 ± 0.2	1.5 ± 0.7
Pb <sup>2+</sup>	-1425	7.9 ± 0.5	4.4 ± 0.2	3.6 ± 0.2	3.5 ± 0.5	1.2 ± 0.2	3.2 ± 0.5

<sup>a</sup> Aqueous phase (10 mL); [Pic<sup>-</sup>] = 2 × 10<sup>-5</sup> M, organic phase (10 mL); [L] = 2 × 10<sup>-4</sup> M, 298 K. <sup>b</sup> Average for three independent extraction experiments.

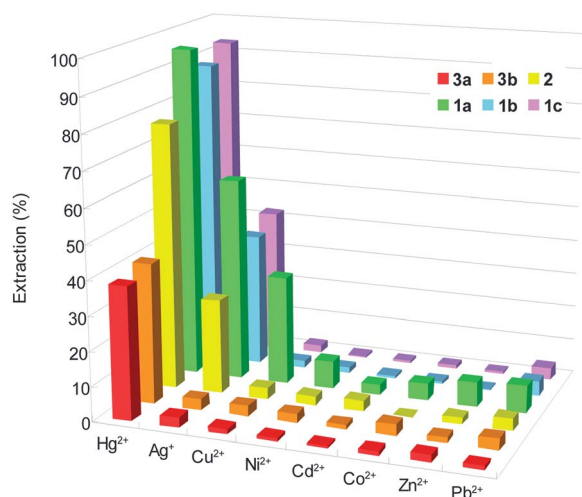


Fig. 8 Extraction of transition metal picrates by compounds **1a–1c**, **2**, **3a** and **3b** from water into dichloromethane at 298 K. Aqueous phase (10 mL); [Pic<sup>-</sup>] = 2 × 10<sup>-5</sup> M, organic phase (10 mL); [L] = 2 × 10<sup>-4</sup> M.

extraction percentage decreased in the order of Hg<sup>2+</sup> > Ag<sup>+</sup> > Cu<sup>2+</sup> > (or ~) Ni<sup>2+</sup> ~ Co<sup>2+</sup> ~ Zn<sup>2+</sup> ~ Pb<sup>2+</sup> ~ Cd<sup>2+</sup>, which does not follow the order of hydration energy<sup>41</sup> or ionic radii of the metal ions<sup>41</sup> (Pb<sup>2+</sup> > Ag<sup>+</sup> > Hg<sup>2+</sup> > Cd<sup>2+</sup> > Zn<sup>2+</sup> ~ Co<sup>2+</sup> > Cu<sup>2+</sup> > Ni<sup>2+</sup>), suggesting that the higher selectivity towards Hg<sup>2+</sup> could be attributed to the synergy of several factors such as hydration of metal ions, ionic radius, charge number and hardness/softness<sup>42</sup> between the nitrogen-containing ligands and Hg<sup>2+</sup>. The effect of structural difference as in **1a–1c**, **2**, **3a** and **3b** upon extraction behaviour was also unraveled by the results from extraction of Ag<sup>+</sup>. Ligand **1a**, **1b**, **1c**, and **2** extracted Ag<sup>+</sup> in 58.7%, 38.5%, 42.1% and 27.4%, respectively; however, the extractability for **3a** and **3b** is very low (<4%), again demonstrating the dependence of extraction upon the presence of intramolecular hydrogen bonds.

Regarding the extraction difference among **1a**, **1b** and **1c** and **2**, electronic effect seems to play a major role, which arises from different substitution position of propoxy groups on benzene rings. *Ortho*- and *para*-substitution provided highest extraction results (95.4% and 93.0%). The efficiency decreased by *ca.* 17%

for compound **2** having no electron-donating groups. Among the four ligands **1a–1c** and **2**, **1c** is not only with high extractability but also much more selective towards extracting Hg<sup>2+</sup> than other metal cations.

To comprehend the complexing behaviour of extracted species in the extraction process, the stoichiometries of the ligands and metal cations were measured. The dependence of log{D/[Pic<sup>-</sup>]<sup>n</sup>} as a function of the concentration of ligands **1a–1c** at constant Hg-picrate concentration offers a linear relationship between log{D/[Pic<sup>-</sup>]<sup>n</sup>} and log[L] with the slopes of 2.26, 1.96 and 2.15 for **1a**, **1b** and **1c**, respectively (Fig. 9). This implicates the presence of the extracted species in approximately 2 : 1 (L : M) between **1a–1c** and Hg<sup>2+</sup>. The values of the extraction constants log K<sub>ex</sub> were calculated to be 17.07, 15.47 and 16.62 for **1a**, **1b** and **1c**, respectively.

Furthermore, the method of Job's plot was used to supply more information on the Hg<sup>2+</sup> binding stoichiometry of **1a–1c**. The resulting Job's plot of **1a/1b/1c–Hg<sup>2+</sup>** complexation is shown in Fig. 10. The maximum absorbance is observed at 0.67, indicating a ligand–metal ratio of 2 : 1 in the complex. On the basis of 2 : 1 stoichiometry and UV-vis titration data (see ESI, Fig. S29–31<sup>†</sup>), the binding constants K<sub>1</sub> and K<sub>2</sub> of **1a–Hg<sup>2+</sup>** in CH<sub>3</sub>CN are estimated to be 3.34 × 10<sup>7</sup> M<sup>-1</sup> and 1.38 × 10<sup>6</sup> M<sup>-1</sup>

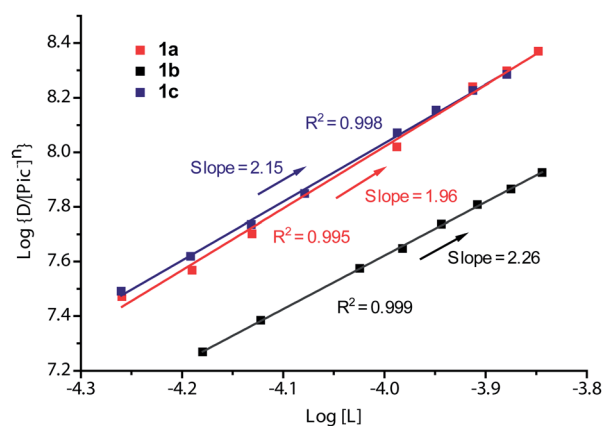


Fig. 9 Plot of log{D/[Pic<sup>-</sup>]<sup>n</sup>} versus log[L] for the extraction of Hg-picrate with ligands **1a–1c**.

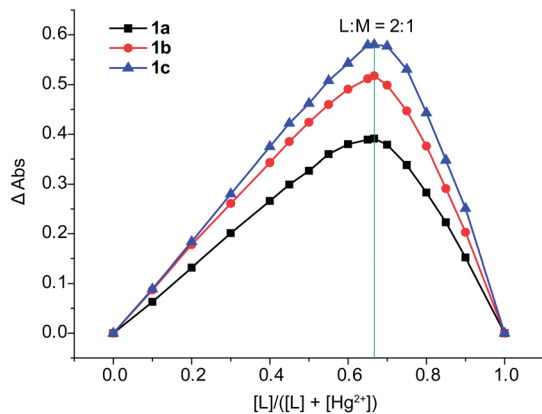


Fig. 10 Job's plot for the determination of stoichiometry in the complex formed by **1a–1c** and  $\text{Hg}^{2+}$  from absorbance measurements in  $\text{CH}_3\text{CN}$ .

(Fig. 11) using nonlinear curve fitting method.<sup>43</sup> Similarly, the binding constants of **1b–Hg**<sup>2+</sup> and **1c–Hg**<sup>2+</sup> are also estimated using the same method (see ESI, Fig. S32 and S33<sup>†</sup>).

To understand the coordinate sites of the ligands, the complex **1a–Hg**<sup>2+</sup> was prepared from a  $\text{CH}_3\text{CN}$  solution containing **1a** and  $\text{Hg}(\text{NO}_3)_2$  in molar ratio 2 : 1 and its infrared spectrum was compared to that of the free ligand **1a** (Fig. 12). The strong band at  $1649\text{ cm}^{-1}$  of  $\nu(\text{C}=\text{O})$  in **1a** shifts to  $1632\text{ cm}^{-1}$  in the complex, a change of  $17\text{ cm}^{-1}$  from vibration of carbonyl oxygen, indicative of the involvement of oxygen atoms in coordination. Since the  $\nu(\text{OC}-\text{N})$  band at  $1264\text{ cm}^{-1}$  for amide bonds in **1a** only shifts upward by  $2\text{ cm}^{-1}$  upon complexation, it suggests that the two amide nitrogens are not involved in the coordination with metal ions. Besides, the band of pyridine ring vibrations appears at  $1475\text{ cm}^{-1}$  in free **1a** and merges into a band at  $1456\text{ cm}^{-1}$  in coordinated **1a**. Based on these observations, we conclude that the coordinate atoms of **1a** should come from carbonyl oxygens, and pyridine nitrogen is also involved.

The complexation of **1a–1c**, **3a** and **3b** with  $\text{Hg}^{2+}$  were evidenced by the spectral change in the <sup>1</sup>H NMR experiments (Fig. 13 and 14). In  $\text{CD}_3\text{CN}/\text{CDCl}_3$  (1/9, v/v), almost all of the protons experience a downfield shift for compound **1a–1c** upon

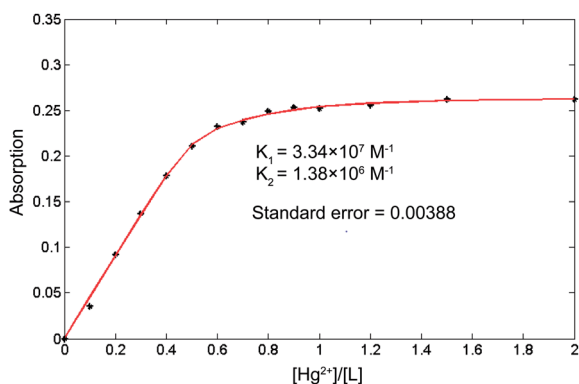


Fig. 11 Curve-fitting analysis for the complexation of **1a** with  $\text{Hg}^{2+}$  in  $\text{CH}_3\text{CN}$ .

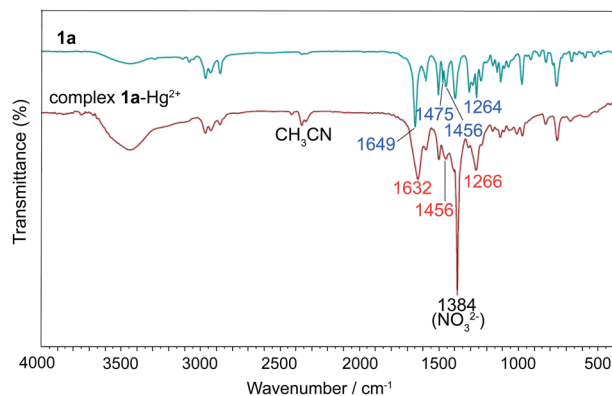


Fig. 12 Infrared spectra of **1a** and the complex **1a–Hg**<sup>2+</sup>.

addition of  $\text{Hg}^{2+}$ . In sharp contrast, for compounds **3a** and **3b**, neither chemical shifts nor signal patterns undergo any change, strongly suggesting that the interaction of **1a–1c** with  $\text{Hg}^{2+}$  is much stronger than that of **3a** or **3b**. This explains the much higher efficiency as indicated for **1a–1c** as extractants compared to **3a** and **3b**. In general, the NMR patterns of **1a–1c** tend to become simple after addition of  $\text{Hg}^{2+}$ . In the case of **1a**, upon complexing the metal ion, though still poorly-resolved, the signal pattern (Fig. 13b) resembles that from variable-temperature <sup>1</sup>H NMR experiments (Fig. 5 at 318 K). For **1b**, the broadened signals change to one set of well-resolved sharp signals in the presence of  $\text{Hg}^{2+}$  (Fig. 13c and d), suggesting the transformation from mixed multiple rotational isomers to only one major isomer induced by introduction of metal ion. The similar result was obtained for **1c**, where minor signals of very low intensity and major signals merge into one set of broad signals at aromatic region (Fig. 13e and f, 6.5–7.6 ppm), while aliphatic protons (0.8–4.2 ppm) become more distinguishable. These results suggest that complexation of  $\text{Hg}^{2+}$  by **1a–1c** facilitate the reduction of possible rotational isomers in solution, but have no influence upon isomerism for

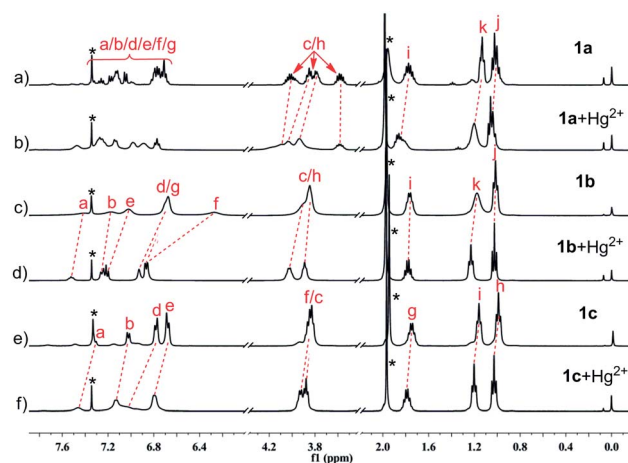


Fig. 13 Partial <sup>1</sup>H NMR spectra in 10%  $\text{CD}_3\text{CN}/90\%$   $\text{CDCl}_3$  (400 MHz, 298 K): (a) **1a**; (b) **1a** +  $\text{Hg}(\text{NO}_3)_2$  (2 : 1); (c) **1b**; (d) **1b** +  $\text{Hg}(\text{NO}_3)_2$  (2 : 1); (e) **1c**; (f) **1c** +  $\text{Hg}(\text{NO}_3)_2$  (2 : 1). Sign "\*" represents signals of solvents.

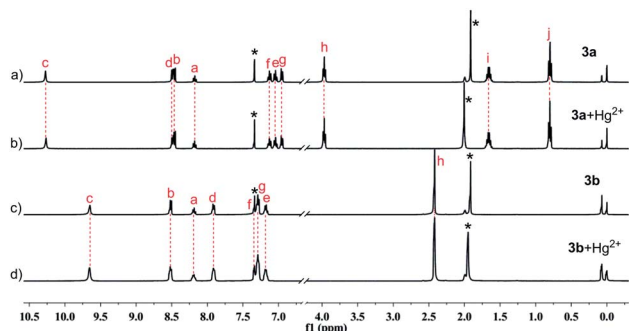


Fig. 14 Partial  $^1\text{H}$  NMR spectra in 10%  $\text{CD}_3\text{CN}/90\%$   $\text{CDCl}_3$  (400 MHz, 298 K): (a) **3a**; (b) **3a** +  $\text{Hg}(\text{NO}_3)_2$  (2 : 1); (c) **3b**; (d) **3b** +  $\text{Hg}(\text{NO}_3)_2$  (2 : 1). Sign "\*" represents signals of solvents.

intramolecularly hydrogen-bonded compounds **3a** and **3b**, again underscoring the importance of hydrogen bonding and rotational isomerism on extraction.

## Experimental

### Materials and reagents

Compounds **4** and **5a–5c** were synthesized following the similar reported procedures.<sup>44,45</sup> Compound **7** was prepared from hydrogenation of **5a** in almost quantitative yield (see ESI<sup>†</sup>). Dichloromethane, picric acid, anhydrous  $\text{Na}_2\text{SO}_4$ ,  $\text{Hg}(\text{NO}_3)_2 \cdot \text{H}_2\text{O}$ ,  $\text{AgNO}_3$ ,  $\text{Cu}(\text{NO}_3)_2 \cdot 3\text{H}_2\text{O}$ ,  $\text{Ni}(\text{NO}_3)_2 \cdot 6\text{H}_2\text{O}$ ,  $\text{Cd}(\text{NO}_3)_2 \cdot 4\text{H}_2\text{O}$ ,  $\text{Zn}(\text{NO}_3)_2 \cdot 6\text{H}_2\text{O}$ ,  $\text{Co}(\text{NO}_3)_2 \cdot 6\text{H}_2\text{O}$ ,  $\text{Pb}(\text{NO}_3)_2$  were the analytical grade reagents and were purchased from Chengdu Kelong Chemical Factory. All other solvents and chemicals used for the synthesis were of reagent grade and used as received.

### Instruments and apparatus

UV-vis spectra were measured by SHIMADZU UV-2350.  $^1\text{H}$  NMR and  $^{13}\text{C}$  spectra were recorded on Bruker AVANCE AV II-400 MHz ( $^1\text{H}$ : 400 MHz;  $^{13}\text{C}$ : 100 MHz). Chemical shifts are reported in  $\delta$  values in ppm and coupling constants ( $J$ ) are denoted in Hz. Multiplicities are denoted as follows: s = singlet, d = doublet, t = triplet, and m = multiplet. High resolution mass data were collected by WATERS Q-TOF Premier.  $\text{CDCl}_3$ ,  $\text{DMSO}-d_6$  and  $\text{CD}_3\text{CN}$  were from Cambridge Isotope Laboratories (CIL).

### Synthesis of compound **6a–6c**

Compound **6a–6c** was synthesized following the reported procedure in a yield of 79%, 81%, 73%, respectively.<sup>27</sup> After two vacuum/ $\text{H}_2$  cycles to remove air from the reaction, the stirred mixture of the nitropropoxybenzene **5a/5b/5c** (1.00 g, 5.52 mmol), 100 mg 10% Pd/C and 50 mL acetonitrile was hydrogenated at ordinary pressure and at room temperature. The reaction was monitored using TLC until the secondary amine was no longer increased. The reaction mixture was filtrated and the filtrate was concentrated under reduced pressure. The crude mixture was purified by flash silica gel column chromatography,

and provided the product as light yellow oil, which was used for the immediate coupling reaction.

### Synthesis of pyridine-based 2,6-dicarboxyamides **1a–1c**, **3a** and **3b**

The general procedure for compounds **1a–1c**, **3a** and **3b** was exemplified by the synthesis of **1a**. Triethylamine (3.35 g, 33.12 mmol) was added into a solution of the amine **6a** (3.32 g, 22.0 mmol) in 100 mL of dry dichloromethane at 0 °C under  $\text{N}_2$ . Pyridine-2,6-dicarbonyl dichloride **4** (2.24 g, 11.0 mmol) was dissolved in 50 mL of dichloromethane and added dropwise to the above mixture. The solution was stirred at room temperature under  $\text{N}_2$  for 4 h. The organic layer was washed with 10% HCl aqueous and followed water, and dried over anhydrous  $\text{Na}_2\text{SO}_4$  and filtered. Most volatiles were removed under reduced pressure and the residue was isolated by precipitation by addition of methanol to give a white solid.

**1a.** Yield 82%.  $^1\text{H}$  NMR (400 MHz,  $\text{CDCl}_3$ )  $\delta$ : 7.35–6.68 (m, 11H, ArH), 4.10–3.95 (m, 2H,  $\text{NCH}_2$ ), 3.88–3.70 (m, 4H,  $\text{OCH}_2$ ), 3.66–3.54 (m, 2H,  $\text{NCH}_2$ ), 1.83–1.68 (m, 4H,  $\text{CH}_2$ ), 1.16–1.12 (m, 6H,  $\text{CH}_3$ ), 1.04–0.96 (m, 6H,  $\text{CH}_3$ ).  $^{13}\text{C}$  NMR (100 MHz,  $\text{CDCl}_3$ )  $\delta$ : 168.14, 167.78, 154.26, 154.22, 153.25, 152.67, 135.42, 135.28, 131.24, 131.09, 130.95, 130.41, 128.49, 128.44, 122.84, 122.37, 120.06, 119.98, 112.01, 111.76, 69.57, 69.50, 43.88, 43.58, 22.59, 12.58, 12.50, 10.71, 10.65. ESI-HRMS ( $m/z$ ) calcd for  $\text{C}_{29}\text{H}_{35}\text{N}_3\text{O}_4$   $[\text{M} + \text{H}]^+$  490.2706,  $[\text{M} + \text{Na}]^+$  512.2525,  $[\text{M} + \text{K}]^+$  528.2265; found  $[\text{M} + \text{H}]^+$  490.2701,  $[\text{M} + \text{Na}]^+$  512.2532,  $[\text{M} + \text{K}]^+$  528.2272.

**1b.** Yield 92%.  $^1\text{H}$  NMR (400 MHz,  $\text{CD}_3\text{COCD}_3$ )  $\delta$ : 7.62 (br s, 1H, PyH), 7.32 (br s, 2H, PyH), 7.10 (s, 2H, ArH), 6.78 (s, 2H, ArH), 6.76 (d,  $J = 8.4$  Hz, 2H, ArH), 6.41 (br s, 2H, ArH), 3.90 (t,  $J = 6.4$  Hz, 4H,  $\text{OCH}_2$ ), 3.85 (br s, 4H,  $\text{NCH}_2$ ), 1.74 (m,  $J = 6.8$  Hz, 4H,  $\text{CH}_2$ ), 1.13 (br s, 6H,  $\text{NCH}_2\text{CH}_3$ ), 1.00 (t,  $J = 7.4$  Hz, 6H,  $\text{CH}_3$ ).  $^{13}\text{C}$  NMR (100 MHz,  $\text{CDCl}_3$ )  $\delta$ : 167.25, 159.56, 153.11, 143.57, 136.12, 129.36, 123.53, 120.50, 114.00, 112.94, 69.60, 45.02, 22.50, 12.80, 10.50. ESI-HRMS ( $m/z$ ) calcd for  $\text{C}_{29}\text{H}_{35}\text{N}_3\text{O}_4$   $[\text{M} + \text{H}]^+$  490.2706,  $[\text{M} + \text{Na}]^+$  512.2525,  $[\text{M} + \text{K}]^+$  528.2265; found  $[\text{M} + \text{H}]^+$  490.2699,  $[\text{M} + \text{Na}]^+$  512.2533,  $[\text{M} + \text{K}]^+$  528.2267.

**1c.** Yield 88%.  $^1\text{H}$  NMR (400 MHz,  $\text{CDCl}_3$ )  $\delta$ : 7.32 (t,  $J = 8.0$  Hz, 1H, PyH), 7.06 (d,  $J = 8.0$  Hz, 2H, PyH), 6.79 (d,  $J = 8.8$  Hz, 4H, ArH), 6.69 (d,  $J = 8.4$  Hz, 4H, ArH), 3.87 (q,  $J = 7.2$  Hz, 4H,  $\text{NCH}_2$ ), 3.83 (t,  $J = 6.4$  Hz, 4H,  $\text{OCH}_2$ ), 1.76 (m,  $J = 6.8$  Hz, 4H,  $\text{CH}_2$ ), 1.17 (t,  $J = 7.0$  Hz, 6H,  $\text{NCH}_2\text{CH}_3$ ), 1.00 (t,  $J = 7.4$  Hz, 6H,  $\text{CH}_3$ ).  $^{13}\text{C}$  NMR (100 MHz,  $\text{CDCl}_3$ )  $\delta$ : 167.35, 157.61, 153.46, 135.67, 134.74, 129.18, 122.99, 114.30, 69.43, 44.77, 22.38, 12.47, 10.35. ESI-HRMS ( $m/z$ ) calcd for  $\text{C}_{29}\text{H}_{35}\text{N}_3\text{O}_4$   $[\text{M} + \text{H}]^+$  490.2706,  $[\text{M} + \text{Na}]^+$  512.2525,  $[\text{M} + \text{K}]^+$  528.2265; found  $[\text{M} + \text{H}]^+$  490.2699,  $[\text{M} + \text{Na}]^+$  512.2528,  $[\text{M} + \text{K}]^+$  528.2269.

**3a.** Yield 81%.  $^1\text{H}$  NMR (400 MHz,  $\text{CDCl}_3$ )  $\delta$ : 10.20 (s, 2H, NH), 8.45 (d,  $J = 7.6$  Hz, 2H, ArH), 8.40 (d,  $J = 8$  Hz, 2H, PyH), 8.09–8.05 (t,  $J = 8$  Hz, 1H, PyH), 7.06–7.03 (t,  $J = 7.2$  Hz, 2H, ArH), 7.00–6.96 (t,  $J = 7.6$  Hz, 2H, ArH), 6.85 (d,  $J = 8$  Hz, 2H, ArH), 3.90–3.87 (t,  $J = 6.4$  Hz, 4H,  $\text{OCH}_2$ ), 1.63–1.54 (m, 4H,  $\text{CH}_2$ ), 0.75–0.71 (t,  $J = 7.6$  Hz, 6H,  $\text{CH}_3$ ).  $^{13}\text{C}$  NMR (100 MHz,  $\text{CDCl}_3$ )  $\delta$ : 160.15, 148.56, 147.25, 138.43, 126.07, 124.05, 123.48, 119.94, 119.14, 109.97, 69.03, 21.20, 9.12. ESI-HRMS ( $m/z$ ) calcd for  $\text{C}_{25}\text{H}_{27}\text{N}_3\text{O}_4$   $[\text{M} + \text{H}]^+$  434.2080,  $[\text{M} + \text{Na}]^+$  456.1899,  $[\text{M} + \text{K}]^+$

472.1639; found  $[M + H]^+$  434.2082,  $[M + Na]^+$  456.1894,  $[M + K]^+$  472.1647.

**3b.** Yield 89%.  $^1H$  NMR (400 MHz,  $CDCl_3$ )  $\delta$ : 9.45 (s, 2H, NH), 8.55 (d,  $J = 7.6$  Hz, 2H, PyH), 8.20–8.16 (t,  $J = 7.6$  Hz, 1H, PyH), 8.16 (d,  $J = 8.0$  Hz, 2H, ArH), 7.34–7.30 (t,  $J = 7.6$  Hz, 2H, ArH), 7.27 (d,  $J = 7.6$  Hz, 2H, ArH), 7.18–7.14 (t,  $J = 7.6$  Hz, 2H, ArH), 2.44 (s, 6H,  $CH_3$ ).  $^{13}C$  NMR (100 MHz,  $CDCl_3$ )  $\delta$ : 160.20, 148.14, 138.56, 129.58, 127.82, 126.00, 124.53, 121.68, 16.96. ESI-HRMS ( $m/z$ ) calcd for  $C_{21}H_{19}N_3O_2$   $[M + H]^+$  346.1556,  $[M + Na]^+$  368.1375,  $[M + K]^+$  384.1114; found  $[M + H]^+$  346.1554,  $[M + Na]^+$  368.1375,  $[M + K]^+$  384.1110.

### Solvent extraction

Heavy metal picrates were prepared by the stepwise addition of  $1 \times 10^{-2}$  M of metal nitrate solution to  $2 \times 10^{-5}$  M aqueous picric acid solution and shaken at 298 K for 1 h. 10 mL of a  $2 \times 10^{-5}$  M aqueous metal picrate solution and 10 mL of a  $2 \times 10^{-4}$  M solution of ligands in  $CH_2Cl_2$  were placed in a stoppered glass tube and vigorously agitated with a mechanical shaker in a thermostated water bath at 298 K for 2 h. The resulting mixtures were left standing for an additional 2 h in order to complete the phase separation. The concentration of the picrate anion remaining in the aqueous phase was determined by UV spectrophotometry at  $\lambda_{max}$  355 nm. Blank experiments showed that no picrate extraction occurred in the absence of ligands. The extractability was determined based on the absorbance of picrate anion in the aqueous solutions. The extractability ( $E\%$ ) was calculated based on the equation:  $E\% = 100(A_0 - A)/A_0$ , where  $A_0$  is the absorbance of the aqueous solution in the absence of ligand,  $A$  is the absorbance of the aqueous phase after extraction. Three independent experiments were carried out and the average value of percent picrate extracted was calculated.

### Conclusion

In summary, a pyridine-based aromatic amides **1a–1c** with *N*-substitution and their analogues **3a** and **3b** containing intramolecular hydrogen bonds were synthesized for probing the interplay of molecular structure and liquid–liquid extraction behaviour towards transition metal ions. X-ray diffraction analysis of ligands **1a** and **3a** provides information of molecular conformation without and with intramolecular H-bonding. The observed *E-anti-anti-E* conformation (**1a**) in the solid state is among one of six reasonable rotational isomeric structures of **1a** optimized by computer modeling. Ordinary and variable-temperature proton and carbon NMR experiments of **1a–1c** disclosed the formation of rotamers due to *N*-substitution. The fact that *N*-substitution is responsible for the higher selectivity and efficiency towards  $Hg^{2+}$  over other metal cations is rationalized by the large difference in rotational restriction between *N*-substituted **1** (**a**, **b** and **c**) and intramolecularly hydrogen bonded **3** (**a**, **b**). The results from  $^1H$  NMR spectra regarding the interaction of the ligands with  $Hg^{2+}$  also verify the extraction difference, and simultaneously disclose the influence of complexation on rotational isomerism of ligands. Despite the absence of intramolecular hydrogen bonding as compounds **1**

(**a**, **b** and **c**), compound **2** still displayed a lower extraction ability than **1** (**a**, **b** and **c**) due to the favorable electronic effect arising from alkoxy substitution. The stoichiometry for the complexation of  $Hg^{2+}$  by **1a–1c** was found to be 2 : 1 (ligand/metal ion) using  $\log\{D/[Pic^-]^n\} - \log[L]$  analysis, Job's plot and UV-vis titration. IR study indicates that the coordinate atoms are carbonyl oxygens and pyridine nitrogen in *N*-substituted ligands. The disclosure of the impact of H-bonding-enforced backbone rigidification and structural variation *via N*-substitution upon extraction as presented in this work may provide in-depth understanding of the extraction process associated with intramolecular hydrogen bonding and rotational conformation.

### Acknowledgements

This work is supported by the National Natural Science Foundation (21172158), NSAF(11076018), the Doctoral Program of the Ministry of Education of China (20130181110023), the National Science Foundation for Fostering Talents in Basic Research of the National Natural Science Foundation of China (J1210004 and J1103315), Open Project of State Key Laboratory of Supramolecular Structure and Materials (SKLSSM201408) and Open Project of State Key Laboratory of Structural Chemistry (20140013). Comprehensive Training Platform of Specialized Laboratory, College of Chemistry, Sichuan University is acknowledged for NMR, HRESI-MS and IR analyses.

### Notes and references

- 1 D. W. Zhang, X. Zhao, J. L. Hou and Z. T. Li, *Chem. Rev.*, 2012, **112**, 5271.
- 2 (a) A. E. V. Gorden, M. A. DeVore, II and B. A. Maynard, *Inorg. Chem.*, 2013, **52**, 3445; (b) B. J. Mincher, G. Modolo and S. P. Mezyk, *Solvent Extr. Ion Exch.*, 2009, **27**, 579.
- 3 (a) H. N. Kim, M. H. Lee, H. J. Kim, J. S. Kim and J. Yoon, *Chem. Soc. Rev.*, 2008, **37**, 1465; (b) I. G. Spiridonov, D. O. Kirsanov, V. A. Babain, M. Y. Alyapyshev, N. I. Eliseev, Y. G. Vlasov and A. V. Legin, *Russ. J. Appl. Chem.*, 2011, **84**, 1354; (c) Ü. Ocak, M. Ocak, X. Shen, K. Surowiec and R. A. Bartsch, *J. Fluoresc.*, 2009, **19**, 997; (d) Ü. Ocak, M. Ocak, K. Surowiec, X. Liu and R. A. Bartsch, *Tetrahedron*, 2009, **65**, 7038; (e) M. A. Qazi, Ü. Ocak, M. Ocak, S. Memon and I. B. Solangi, *J. Fluoresc.*, 2013, **23**, 575.
- 4 (a) P. Geoghegan and P. O'Leary, *ACS Catal.*, 2012, **2**, 573; (b) N. Kumagai and M. Shibasaki, *Angew. Chem., Int. Ed.*, 2013, **52**, 223.
- 5 S. A. Ansari, P. Pathak, P. K. Mohapatra and V. K. Manchanda, *Chem. Rev.*, 2012, **112**, 1751.
- 6 (a) A. Casnati, N. Della Ca', M. Fontanella, F. Sansone, F. Ugozzoli, R. Ungaro, K. Liger and J. F. Dozol, *Eur. J. Org. Chem.*, 2005, 2338; (b) E. Macerata, F. Sansone, L. Baldini, F. Ugozzoli, F. Brisach, J. Haddaoui, V. Hubscher-Bruder, F. Arnaud-Neu, M. Mariani, R. Ungaro and A. Casnati, *Eur. J. Org. Chem.*, 2010, 2675; (c) M. Galletta, L. Baldini, F. Sansone, F. Ugozzoli, R. Ungaro, A. Casnati and M. Mariani, *Dalton Trans.*, 2010, **39**, 2546.

- 7 (a) M. M. Reinoso-García, D. Jańczewski, D. N. Reinhoudt, W. Verboom, E. Malinowska, M. Pietrzak, C. Hill, J. Bába, B. Grüner, P. Selucky and C. Grüttner, *New J. Chem.*, 2006, **30**, 1480; (b) K. Matloka, A. K. Sah, M. W. Peters, P. Srinivasan, A. V. Gelis, M. Regalbuto and M. J. Scott, *Inorg. Chem.*, 2007, **46**, 10549; (c) E. V. Sharova, O. I. Artyushin, A. N. Turanov, V. K. Karandashev, S. B. Meshkova, Z. M. Topilova and I. L. Odinets, *Cent. Eur. J. Chem.*, 2012, **10**, 146.
- 8 (a) A. Shimada, T. Yaita, H. Narita, S. Tachimori and K. Okuno, *Solvent Extr. Ion Exch.*, 2004, **22**, 147; (b) M. Y. Alyapyshev, V. A. Babain, N. E. Borisova, R. N. Kiseleva, D. V. Safronov and M. D. Reshetova, *Mendeleev Commun.*, 2008, **18**, 336; (c) A. Paulenova, M. Y. Alyapyshev, V. A. Babain, R. S. Herbst and J. D. Law, *Sep. Sci. Technol.*, 2008, **43**, 2606; (d) M. Y. Alyapyshev, V. A. Babain, L. I. Tkachenko, A. Paulenova, A. A. Popova and N. E. Borisova, *Solvent Extr. Ion Exch.*, 2014, **32**, 138.
- 9 (a) J. C. Noveron, M. M. Olmstead and P. K. Mascharak, *J. Am. Chem. Soc.*, 2001, **123**, 3247; (b) T. C. Harrop, L. A. Tyler, M. M. Olmstead and P. K. Mascharak, *Eur. J. Inorg. Chem.*, 2003, 475; (c) R. Kapoor, A. Kataria, A. Pathak, P. Venugopalan, G. Hundal and P. Kapoor, *Polyhedron*, 2005, **24**, 1221; (d) R. Kapoor, A. Kataria, P. Kapoor and P. Venugopalan, *Transition Met. Chem.*, 2004, **29**, 425; (e) R. Kapoor, A. Kataria, P. Venugopalan and P. Kapoor, *Inorg. Chem.*, 2004, **43**, 6699.
- 10 (a) D. O. Kirsanov, N. E. Borisova, M. D. Reshetova, A. V. Ivanov, L. A. Korotkov, I. I. Eliseev, M. Y. Alyapyshev, I. G. Spiridonov, A. V. Legin, Y. G. Vlasov and V. A. Babain, *Russ. Chem. Bull., Int. Ed.*, 2012, **61**, 881; (b) J. L. Lapka, A. Paulenova, M. Y. Alyapyshev, V. A. Babain, R. S. Herbst and J. D. Law, *J. Radioanal. Nucl. Chem.*, 2009, **280**, 307.
- 11 (a) A. Fujiwara, Y. Nakano, T. Yaita and K. Okuno, *J. Alloys Compd.*, 2008, **456**, 429; (b) J. L. Lapka, A. Paulenova, L. N. Zakharov, M. Y. Alyapyshev and V. A. Babain, *IOP Conf. Ser.: Mater. Sci. Eng.*, 2010, **9**, 012029.
- 12 V. A. Babain, M. Y. Alyapyshev, I. V. Smirnov and A. Y. Shadrin, *Radiochemistry*, 2006, **48**, 369.
- 13 (a) H. Stephan, K. Gloe, J. Beger and P. Mühl, *Solvent Extr. Ion Exch.*, 1991, **9**, 435; (b) Y. Sasaki and G. R. Choppin, *Anal. Sci.*, 1996, **12**, 225.
- 14 M. Y. Alyapyshev, V. A. Babain, L. I. Tkachenko, I. I. Eliseev, A. V. Didenko and M. L. Petrov, *Solvent Extr. Ion Exch.*, 2011, **29**, 619.
- 15 (a) S. L. Li, T. Xiao, C. Lin and L. Wang, *Chem. Soc. Rev.*, 2012, **41**, 5950; (b) L. Yuan, P. Zhang, W. Feng and B. Gong, *Curr. Org. Chem.*, 2011, **15**, 1250; (c) P. K. Baruah and S. Khan, *RSC Adv.*, 2013, **3**, 21202; (d) P. A. Gale, N. Busschaert, C. J. E. Haynes, L. E. Karagiannidis and I. L. Kirby, *Chem. Soc. Rev.*, 2014, **43**, 205.
- 16 (a) Z. Shirin, J. Thompson, L. Liable-Sands, G. P. A. Yap, A. L. Rheingold and A. S. Borovik, *J. Chem. Soc., Dalton Trans.*, 2002, 1714; (b) J. R. Turkington, P. J. Bailey, J. B. Love, A. M. Wilson and P. A. Tasker, *Chem. Commun.*, 2013, **49**, 1891.
- 17 X. Yang, L. Chen, Y. Yang, Y. He, S. Zou, W. Feng, Y. Yang, N. Liu, J. Liao and L. Yuan, *J. Hazard. Mater.*, 2012, **217–218**, 171.
- 18 (a) L. Yang, L. Zhong, K. Yamato, X. Zhang, W. Feng, P. Deng, L. Yuan, X. C. Zeng and B. Gong, *New J. Chem.*, 2009, **33**, 729; (b) W. Feng, K. Yamato, L. Yang, J. S. Ferguson, L. Zhong, S. Zou, L. Yuan, X. C. Zeng and B. Gong, *J. Am. Chem. Soc.*, 2009, **131**, 2629; (c) Y. Yang, W. Feng, J. Hu, S. Zou, R. Gao, K. Yamato, M. Kline, Z. Cai, Y. Gao, Y. Wang, L. Li, Y. Ynag, L. Yuan, X. C. Zeng and B. Gong, *J. Am. Chem. Soc.*, 2011, **133**, 18590; (d) J. Hu, L. Chen, Y. Ren, P. Deng, X. Li, Y. Wang, Y. Jia, J. Luo, X. Yang, W. Feng and L. Yuan, *Org. Lett.*, 2013, **15**, 4670.
- 19 L. Zhong, L. Chen, W. Feng, S. Zou, Y. Yang, N. Liu and L. Yuan, *J. Inclusion Phenom. Macrocyclic Chem.*, 2012, **72**, 367.
- 20 L. He, Q. Jiang, Y. Jia, Y. Fang, S. Zou, Y. Yang, J. Liao, N. Liu, W. Feng, S. Luo, Y. Yang, L. Yang and L. Yuan, *J. Chem. Technol. Biotechnol.*, 2013, **88**, 1930.
- 21 H. Chu, L. He, Q. Jiang, Y. Fang, Y. Jia, X. Yuan, S. Zou, X. Li, W. Feng, Y. Yang, N. Liu, S. Luo, Y. Yang, L. Yang and L. Yuan, *J. Hazard. Mater.*, 2014, **264**, 211.
- 22 (a) J. L. Lapka, A. Paulenova, M. Y. Alyapyshev, V. A. Babain, J. D. Law and R. S. Herbst, *IOP Conf. Ser.: Mater. Sci. Eng.*, 2010, **9**, 012068; (b) J. L. Lapka, A. Paulenova, R. S. Herbst and J. D. Law, *Sep. Sci. Technol.*, 2010, **45**, 1706; (c) M. Y. Alyapyshev, V. A. Babain, L. I. Tkachenko, I. I. Eliseev, A. V. Didenko and M. L. Petrov, *Solvent Extr. Ion Exch.*, 2011, **29**, 619; (d) A. Paulenova, M. Y. Alyapyshev, V. A. Babain, R. S. Herbst and J. D. Law, *Solvent Extr. Ion Exch.*, 2013, **31**, 184.
- 23 (a) M. Alyapyshev, V. Babain, N. Borisova, I. Eliseev, D. Kirsanov, A. Kostin, A. Legin, M. Reshetova and Z. Smirnova, *Polyhedron*, 2010, **29**, 1998; (b) T. L. Borgne, J. M. Bénech, S. Floguet, G. Bernardinelli, C. Aliprandini, P. Bettens and C. Piguet, *Dalton Trans.*, 2003, 3856.
- 24 L. Wu, Y. Fang, Y. Jia, Y. Yang, J. Liao, N. Liu, X. Yang, W. Feng, J. Ming and L. Yuan, *Dalton Trans.*, 2014, **43**, 3835.
- 25 (a) V. A. Babain, M. Y. Alyapyshev and R. N. Kiseleva, *Radiochim. Acta*, 2007, **95**, 217; (b) E. Makrlík, P. Vaňura, P. Selucký, V. A. Babain and M. Y. Alyapyshev, *Radiochemistry*, 2009, **51**, 479; (c) D. O. Kirsanov, O. V. Mednova, E. N. Pol'shin, A. V. Legin, M. Y. Alyapyshev, I. I. Eliseev, V. A. Babain and Y. G. Vlasov, *Russ. J. Appl. Chem.*, 2009, **82**, 247; (d) E. Makrlík, P. Vaňura, P. Selucký, V. A. Babain and I. V. Smirnov, *J. Radioanal. Nucl. Chem.*, 2010, **283**, 839; (e) M. Y. Alyapyshev, V. A. Babain, L. I. Tkachenko, I. I. Eliseev, A. V. Didenko and M. L. Petrov, *Solvent Extr. Ion Exch.*, 2011, **29**, 619; (f) D. Kirsanov, A. Legin, M. Tkachenko, I. Surzhina, M. Khaidukova and V. Babain, *AIP Conf. Proc.*, 2011, **1362**, 104.
- 26 M. Y. Alyapyshev, V. A. Babain, Y. A. Pokhitonov and V. M. Esimantovskiy, *Adv. Nucl. Fuel Cycles Syst.*, 2007, 1836.
- 27 H. Sajiki, T. Ikawa and K. Hirota, *Org. Lett.*, 2004, **6**, 4977.
- 28 (a) T. J. Bartczak, Z. M. Michlska, B. Ostaszewski, P. Sobota and K. Strzelec, *Inorg. Chim. Acta*, 2001, **319**, 229; (b)

- D. S. Marlin, M. M. Olmstead and P. K. Mascharak, *J. Mol. Struct.*, 2000, **554**, 211; (c) A. Itai, Y. Toriumi, S. Saito, H. Kagechika and K. Shudo, *J. Am. Chem. Soc.*, 1992, **114**, 10649.
- 29 (a) Q. Y. Yang, Z. Y. Zhou and J. Y. Qi, *Acta Crystallogr.*, 2001, **E57**, o1161; (b) M. F. Mayer, S. Nakashima and S. C. Zimmerman, *Org. Lett.*, 2005, **7**, 3005; (c) X. Li, Y. Jia, Y. Ren, Y. Wang, J. Hu, T. Ma, W. Feng and L. Yuan, *Org. Biomol. Chem.*, 2013, **11**, 6975.
- 30 (a) B. Dolenský, R. Konvalinka, M. Jakubek and V. Král, *J. Mol. Struct.*, 2013, **1035**, 124; (b) J. G. Sośnicki and P. E. Hansen, *J. Mol. Struct.*, 2004, **700**, 91.
- 31 Y. Hamuro, S. J. Geib and A. D. Hamilton, *J. Am. Chem. Soc.*, 1996, **118**, 7529.
- 32 (a) W. E. Stewart and T. H. Siddall III, *Chem. Rev.*, 1970, **70**, 517; (b) N. Ototake, T. Taguchi and O. Kitagawa, *Tetrahedron Lett.*, 2008, **49**, 5458; (c) J. S. Laursen, J. Engel-Andreasen, P. Fristrup, P. Harris and C. A. Olsen, *J. Am. Chem. Soc.*, 2013, **135**, 2835.
- 33 (a) B. Gong, *Acc. Chem. Res.*, 2008, **41**, 1376; (b) L. Yuan, W. Feng, K. Yamato, A. R. Sanford, D. Xu, H. Guo and B. Gong, *J. Am. Chem. Soc.*, 2004, **126**, 11120.
- 34 J. F. Malone, C. M. Murray, G. M. Dolan, R. Docherty and A. J. Lavery, *Chem. Mater.*, 1997, **9**, 2983.
- 35 B. Klepetářová, E. Makrlík, V. A. Babain and V. Kašička, *Acta Crystallogr.*, 2012, **E68**, o1099.
- 36 (a) N. H. Shah, G. L. Butterfoss, K. Nguyen, B. Yoo, R. Bonneau, D. L. Rabenstein and K. Kirshenbaum, *J. Am. Chem. Soc.*, 2008, **130**, 16622; (b) B. F. Pedersen and B. Pedersen, *Tetrahedron Lett.*, 1965, **34**, 2995; (c) R. Yamasaki, A. Tanatani, I. Azumaya, S. Saito, K. Yamaguchi and H. Kagechika, *Org. Lett.*, 2003, **5**, 1265.
- 37 M. J. Frisch, G. W. Trucks, H. B. Schlegel, G. E. Scuseria, M. A. Robb, J. R. Cheeseman, V. G. Zakrzewski, J. A. Montgomery, Jr, R. E. Stratmann, J. C. Burant, S. Dapprich, J. M. Millam, A. D. Daniels, K. N. Kudin, M. C. Strain, O. Farkas, J. Tomasi, V. Barone, M. Cossi, R. Cammi, B. Mennucci, C. Pomelli, C. Adamo, S. Clifford, J. Ochterski, G. A. Petersson, P. Y. Ayala, Q. Cui, K. Morokuma, N. Rega, P. Salvador, J. J. Dannenberg, D. K. Malick, A. D. Rabuck, K. Raghavachari, J. B. Foresman, J. Cioslowski, J. V. Ortiz, A. G. Baboul, B. B. Stefanov, G. Liu, A. Liashenko, P. Piskorz, I. Komaromi, R. Gomperts, R. Martin, L. D. J. Fox, T. Keith, M. A. Al-Laham, C. Y. Peng, A. Nanayakkara, M. Challacombe, P. M. W. Gill, B. Johnson, W. Chen, M. W. Wong, J. L. Andres, C. Gonzalez, M. Head-Gordon, E. S. Replogle and J. A. Pople, Gaussian Inc., Wallingford, CT, 2004.
- 38 (a) M. Ocak, H. Alp, H. Kantekin, H. Karadeniz and Ü. Ocak, *J. Inclusion Phenom. Macrocyclic Chem.*, 2008, **60**, 17; (b) H. Alp, M. Ocak, M. Özdemir and Ü. Ocak, *Sep. Sci. Technol.*, 2006, **41**, 3039; (c) Ü. Ocak, H. Alp, P. Gökçe and M. Ocak, *Sep. Sci. Technol.*, 2006, **41**, 391; (d) Ü. Ocak, Y. Gök and H. B. Şentürk, *Sep. Sci. Technol.*, 2009, **44**, 1240.
- 39 P. Kapoor, A. Kumar, J. Nistandra and P. Venugopalan, *Transition Met. Chem.*, 2000, **25**, 465.
- 40 M. Iqbal, P. K. Mohapatra, S. A. Ansari, J. Huskens and W. Verboom, *Tetrahedron*, 2012, **68**, 7840.
- 41 Y. Marcus, *J. Chem. Soc., Faraday Trans.*, 1991, **87**, 2995.
- 42 (a) H. Alp, H. Z. Gök, H. Kantekin and Ü. Ocak, *J. Hazard. Mater.*, 2008, **159**, 519; (b) N. Singh and D. O. Jang, *J. Hazard. Mater.*, 2009, **168**, 727.
- 43 P. Thordarson, *Chem. Soc. Rev.*, 2011, **40**, 1305.
- 44 Y. Y. Zhu, C. Cui, N. Li, B. W. Wang, Z. M. Wang and S. Gao, *Eur. J. Org. Chem.*, 2013, **17**, 3101.
- 45 J. S. Bae and H. S. Freeman, *Fibers Polym.*, 2002, **3**, 140.